

A CRITICAL REVIEW OF TRIAXIALITY BASED FAILURE CRITERIA

G. Maresca, P. P. Milella, G. Pino

ANPA - Via V. Brancati, Roma

SUMMARY: Curves providing a failure strain value depending on a local triaxiality factor have been obtained experimentally by a number of investigators and are usually applied in the structural analysis. In this paper, the experimental and theoretical bases of this practice are reviewed. Results obtained in a campaign performed on cruciform specimens at the Joint Research Center of Ispra are also considered. The possible dependence of the failure strain on the whole history of the local triaxiality and on parameters other than triaxiality is explored. Finally, experimental difficulties in checking the available failure theories are shortly discussed.

KEYWORDS: triaxiality, ductility reduction, voids growth.

INTRODUCTION

It is well known that a triaxial stress state reduces locally the ductility of structural materials. Ductility reduction is also produced by low temperatures and high strain rates. In this paper we are interested in the effect of triaxiality on ductility of materials working at room temperature or at temperatures of about 300÷400 °C. As far as it concerns strain rates, our discussion will be limited to values in the range between 10^{-4} and 10^{-2} sec^{-1} . Experimental curves relating a variable representing the local triaxiality with the local reduction in ductilities have been provided by many investigators. A typical curve (Fig. 1) is the one from Manjoine (Manjoine, 1982) relating the Davis Triaxiality Factor (TFD), defined as

$$TFD = \frac{\sqrt{2} \cdot (s_1 + s_2 + s_3)}{\sqrt{(s_1 - s_2)^2 + (s_2 - s_3)^2 + (s_3 - s_1)^2}}$$

with the ductility reduction, defined as

$$\frac{e_r}{e_r} = 2^{(1-TFD)}$$

where, in the above formula,

e_r =equivalent strain

e_r =elongation at rupture by the uniaxial test.

This curve has been based on the conservative enveloping of experimental tests. It has been adopted by EPRI as a failure criterion to be used in design (Dameron et alii, 1991).

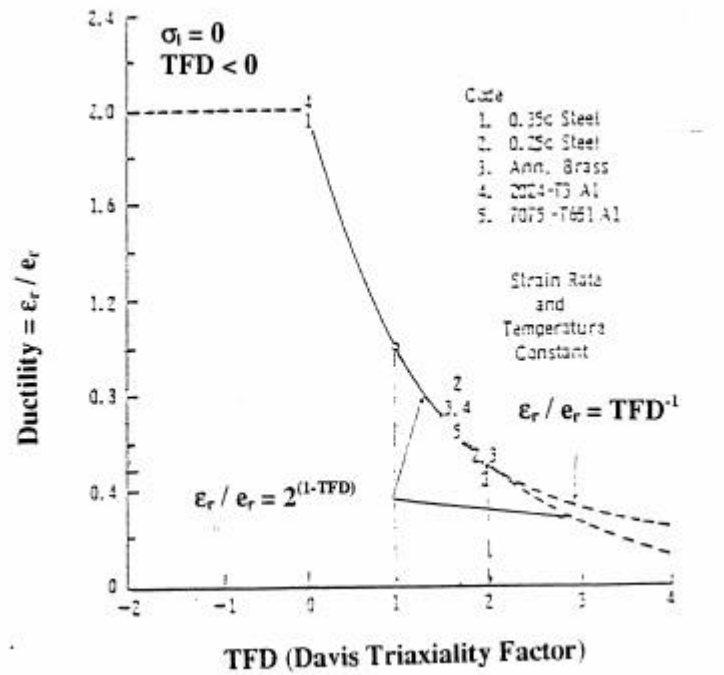


Fig. 1: Ductility criteria for failure as proposed in Manjoine, 1982.

The adoption of the above curve is justified by its conservatism. However, when a more precise representation of the state of affairs is wished, some ambiguities in the Manjoine curve must be pointed out and solved. The typical application we are thinking about is the optimization of the design of penetrations in large containment vessels loaded by internal pressure. Usually, in this case, relevant triaxiality is found at the junction between nozzles or hatches reinforcement plates and the vessel shell.

The failure of the containment because of an increase in the loading may occur at different locations mainly for two different reasons: plastic instability or ductility reduction at the triaxially stressed points. A well balanced design, against extreme loading conditions, require that the failure level for these two different failure modes be approximately the same. This presupposes the ability of the designer to determine with approximately the same accuracy the failure level in both cases. Presently this is not what happens: while the plastic instability level can be determined with some accuracy, the same does not happen for the effects of triaxiality, because of experimental and theoretical complications in the correlation of these effects with the local stress and strain state.

The present generation of computers allows to represent at a high degree of fidelity the elastic-plastic behavior of a containment vessel. The main limitation often stays in the insufficient knowledge of the real stress-strain curve of the material and, more in general, in the insufficient knowledge of the real behavior of the material, as far as it concerns deformation and fracture. Therefore, there is room to improve the models of the material up to the complete utilization of the computers capacity getting a substantial improvement in the ultimate strength of containment structures. This means, for a pressure boundary of a given thickness, an improvement in the design of penetrations, reinforcements and other singularities.

Thinking about specimens, the ductility can be represented, in general, by the maximum equivalent strain which can be reached in a given loading configuration. Really, we refer to displacement controlled conditions. In the case of force controlled conditions instability phenomena usually occurs before the occurrence of a failure strain. This is not always the case because, for very high triaxiality and consequent strong reduction in ductility, the failure may occur before the occurrence of instability. As far as it concerns containment vessels, the failure by plastic instability is produced by a primary load. Local ductility reduction may affect the ductility of the material in the fore-necking region (with reference to the engineering stress-strain curve) as well as the after necking region. This latest case happens when relevant secondary stresses are produced in the neighbouring of penetrations.

EFFECTS OF TRIAXIALITY

According to the present knowledge of the materials behavior stress triaxiality can affect the rupture mainly by two ways. The first is simply preventing the plastic deformation (which depends on stress deviatorics) while the level of the stress increases. Finally a rupture stress is reached and a rupture by cleavage is obtained. The other mechanism is by producing a void growth inside the material. Preexisting inclusions inside the materials originate microvoids which, because of plastic straining, are enlarged in a way that is supported by local triaxiality until void coalescence and anticipated ductile rupture occurs. This double nature of the failure by triaxiality makes difficult to represent by a unique curve the relationship between stress triaxiality and local ductility reduction.

The Davis Triaxiality Factor is proportional to the ratio between the first and the second invariant of the local Cauchy stress tensor. A number of models of ductile failure try to relate this factor to the void growth inside the material. The first one is probably the model studied by McClintok (McClintok, 1968). Improvements are due to Rice and Tracey (Rice and Tracey, 1969) and Gurson (Gurson, 1977).

In each one of these models macroscopic stresses and strains are related to microscopic stress and strain fields around the voids. The void growth is then represented by a void size parameter, which does not represent possible changes in the voids shape and requires that the evolution of macroscopic stresses and strains be limited by appropriate conditions. This lack of generality obviously reflects in a limited applicability to real structures where the variety of geometry and loading conditions go beyond the range covered by the theory. These limits also reflect in the experimental verifications where the local loading and straining of specimens cannot be completely controlled.

Available experimental data have been obtained in a number of ways. Multiaxial stresses can be obtained, for example, by

- thin walled cylindrical specimens under combination of tension, torsion, internal and external pressure, open and closed end specimens,
- cruciform loading of plate specimens,
- notched specimens (round or prismatic),
- plate-type specimens such as bulging plate, wide cantilever plate (beam) and rhombic plate under bending,
- pressurized thick walled tubes.

Notice that, because of necking, also in the uniaxial testing of unnotched specimens information regarding the behaviour of the material under triaxial conditions can be obtained. Infact at the necked section of the specimen an hydrostatic stress growing from the periphery to the axis exists, and a certain amount of triaxiality is obtained at the center of the specimen. When the combination of tension, torsion, internal and external pressure, is applied, a wide range of triaxial conditions can be explored controlling the pressure, the axial load F and the torque M :

$$S_x = \frac{4F}{\rho(D_o^2 - D_i^2)}$$
$$S_y = \frac{2(p_i - p_o)(D_o - D_i)}{2(D_o - D_i)}$$
$$S_z \approx -\frac{p_i + p_o}{2}$$
$$t_{xy} = \frac{M}{2\rho R_m^2 t}$$

In order to relate the local triaxiality with the ductility reduction, tests must be made creating a given triaxiality, or triaxiality pattern inside the specimen, and the local strain at rupture must be determined. This experimental program require to be performed that

1. The point of rupture initiation is determined.
2. The history of the local stress distribution at the rupture point is determined.
3. The final strain state at the rupture point immediately before the rupture is also determined.

Under a given load configuration the local triaxiality is affected by the local geometry and by changes in geometry. These changes can be very relevant according to the amount of necking which is cumulated before the rupture initiation. Finally, the geometry of the specimen may affect the geometry change and the necking extension.

The main effect of local necking is a macroscopic alteration of the local geometry leading to a change in the stress pattern. The appearance of necking depends on the geometry of the structure. In usual cases it occurs in the form of plastic instability. Diffuse necking also can occur but it is not interesting from our point of view as it does not affect the stress pattern. Diffuse necking does not alterate the local TFD (geometrical TFD).

THE UNIAXIAL TENSION TEST

The uniaxial test, performed on cylindrical or prismatic specimens, is the most common way to characterize a material. Usually the test is performed according to displacement imposed conditions and the load versus the applied displacement is measured providing the usual engineering stress-engineering strain diagrams.

However, plastic calculations, to be performed according to the Prandtl-Reuss incremental theory, require the use of a universal stress-strain curve based on the logarithmic strain. To pass from the conventional strain to the logarithmic strain the transformation

$$e_T = \ln(1 + e_c)$$

must be applied. It can also be shown that a true stress can be computed as

$$s_T = s_c \cdot (1 + e_c)$$

Therefore a curve relating the logarithmic strain to the true stress can be obtained from the engineering stress-strain curve. This curve is correct only before the necking point. After the necking, the stress is no longer constant in the necked section of the specimen: in this section, only the average stress can be measured and obviously it is greater than in other sections. Moreover, although the assumption of constant axial strain in each given section is usually made, the axial strain value changes from section to section being greater in the necked section. So the final elongation at rupture does not represent a local value of the strain but only an average along the axis of the specimen. To extrapolate the stress-strain relationship in the post-necking region some assumptions must be made. First of all it is known from experiments performed by Mc Gregor and Davidenkov that a linear relationship exists between the average stress in the necked section and the logarithmic strain. Furthermore, the stress distribution in the necked section has been evaluated by Bridgman as a function of the negative surface curvature at the periphery of the necked section. Therefore, an assumption regarding the dependence of the curvature on the logarithmic strain, or, better, a measure of the evolution of this parameter during the test, allows to evaluate the stress distribution in the necked section as the deformation progresses. By this way a final true strain at failure can be obtained. Notice that the rupture occurs at the center of the specimen. According to Bridgman the stress distribution in the round specimen is provided by

$$s_z = s_{average} \cdot \left(1 + \ln \left(1 + \frac{a^2 + 2aR - r^2}{2aR} \right) \right)$$

$$s_r = s_q = s_{average} \cdot \ln \left(\frac{a^2 + 2aR - r^2}{2aR} \right)$$

As far as it concerns the strain, at each point it results $\sigma_r = \sigma_\theta$ and it is also $\varepsilon_r = \varepsilon_\theta$. But it is $\varepsilon_z + \varepsilon_r + \varepsilon_\theta = 0$ because of the volume conservation assumption. Thus the equivalent strain is the same in each point of the section as well as the equivalent stress. However a hydrostatic strain growing as the axis is approached is superposed to the stress deviatorics. By this way also the TFD grows approaching the specimen axis from a value 1 at the periphery to a value equal to

$$TFD = 3 \left(1 + \ln \frac{a}{2R} \right)$$

at the center of the specimen.

Really, what we can learn from the unnotched tensile specimen is that a failure strain is reached at the maximum TFD location. This location stays in the center of the necked section of the specimen. According to this kind of test we can also conclude that for $TFD=1$ the local failure strain must be greater than the strain reached at the end of the test. In fact, at the periphery of the necked section, the value 1 of the TFD is maintained for all the test duration and the equivalent strain is the same in the whole necked section. Different steels, as well as other metals, may show a more or less marked sensitivity to necking. When the rupture occurs without large necking R is very high and a TFD value approximately equal to 1 is obtained also at the specimen center.

A measure of the relevance of necking can be obtained comparing the logarithmic elongation at rupture (logarithm of the ratio between the final gauge length and the initial one) with the logarithm of the ratio between the initial and the final area in the necked section.

TESTS BY NOTCHED SPECIMENS

To get data related to a given triaxiality factor notched specimen may be used. In this case round or prismatic specimen may be used. Notice that in this latest case the formula are referred to the given geometry. However also in this case the geometry changes as the test progresses and the final value should be used.

Data relating the failure strain versus TFD are available. For example in Fig. 1 data from Manjoine are reported. These data have been normalized to the rupture elongation of the material as it can be obtained in the uniaxial test. Notice that an ambiguity exists because to specify the rupture elongation also the size of the specimen and the gauge length must be specified. These data are well approximated by the curve $2^{(1-TFD)}$. Notice that this curve passes through the point $TFD=1$ and $\epsilon_r/\epsilon_t=1$. While conservative, no physical reason exists for this behavior. At the $TFD=1$ point the ductility reduction provided by the above curve is very far from what is obtained by the unnotched specimen uniaxial test.

TESTS BY CRUCIFORM SPECIMENS

Computer assisted testing of plane stress cruciform specimens have been used to evaluate the failure strain in carbon steel under plane stress biaxial loading. The tests were carried out at the Ispra Laboratories by a low velocity biaxial machine. Strain values at failure which are about 50% of the corresponding uniaxial test value (140%) were obtained.

A typical specimen after the rupture is shown in Fig. 2. Notice the small cavity which has been set up at the center of the specimen in order to get a strong local amplification of the strain. A simple calculation is able to show that this amplification is a consequence of volume conservation in plastic deformation. This is confirmed by more sophisticated finite element models. The tests have been completely reproduced using the structural computer code MARC. By this way the pattern of stresses and strains inside the specimen as the deformation progresses can be determined and correlated to the parameters measured during the test. Applying at the model the same displacements reached at the periphery of the specimen during the test, the measured increase of the cavity diameter results to be exactly reproduced by calculation. This validates the adequacy of the model which is then used to evaluate the strains reached in the specimen

at the rupture point. The calculated strain value is finally confirmed by the thickness reduction measured at the rupture location. Obviously it is required a good reproduction of the real stress-strain curve specially in the post necking region, although the displacement controlled condition characterizing the test partially forgives small discrepancies.

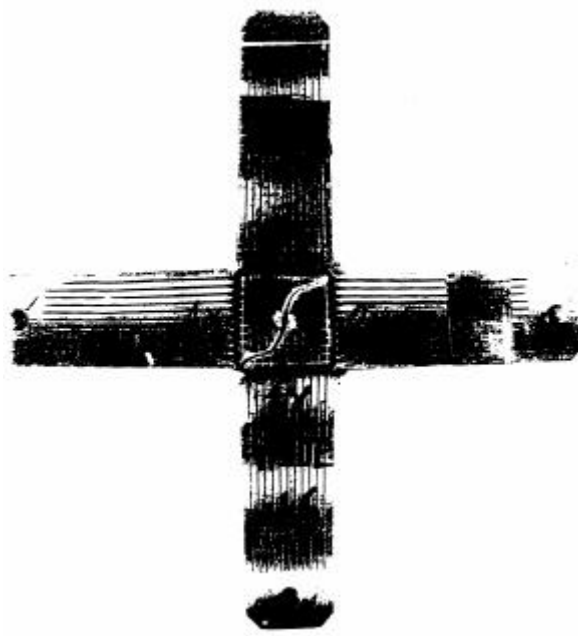


Fig. 2: Ductile rupture of a cruciform specimen biaxially loaded. Ispra tests, 1996.

The obtained results have been compared with results obtained by the punch method and by the Ghosh theory (Ghosh, 1976). The typical Ghosh diagrams is reported in Fig. 3. Notice that in the diagram the equivalent strain, the failure strain according to the criteria proposed by Manjoine and the TFD values are also reported

The Ghosh theory is a particularization of the Rice and Tracey model of void growth to the case of sheets loaded in plane stress conditions. However the final rupture mechanism is different from the one proposed by McClintock or Rice and Tracey. In fact it is based on the appearance of shear links between the voids as they are sufficiently enlarged. The good agreement with experimental data regarding sheets, get one to think that this mechanism is really active in the plane stress conditions.

ISO-TFD CURVES

Fig. 4 shows a family of iso-TFD curves. In the figure the x axis represent the σ_2/σ_1 ratio while the y axis represent the σ_3/σ_1 ratio, being σ_1 , σ_2 , and σ_3 the three principal stresses and $|\sigma_1|$ the maximum absolute value. According to these assumptions x and y range from -1 to +1. The isoTFD curves can be determined by the equation

$$TFD = \frac{\sqrt{2} \cdot (1 + x + y)}{\sqrt{(1-x)^2 + (1-y)^2 + (y-x)^2}}$$

which, for a fixed TFD value represent an ellipsis with an axis on the line $x=y$.

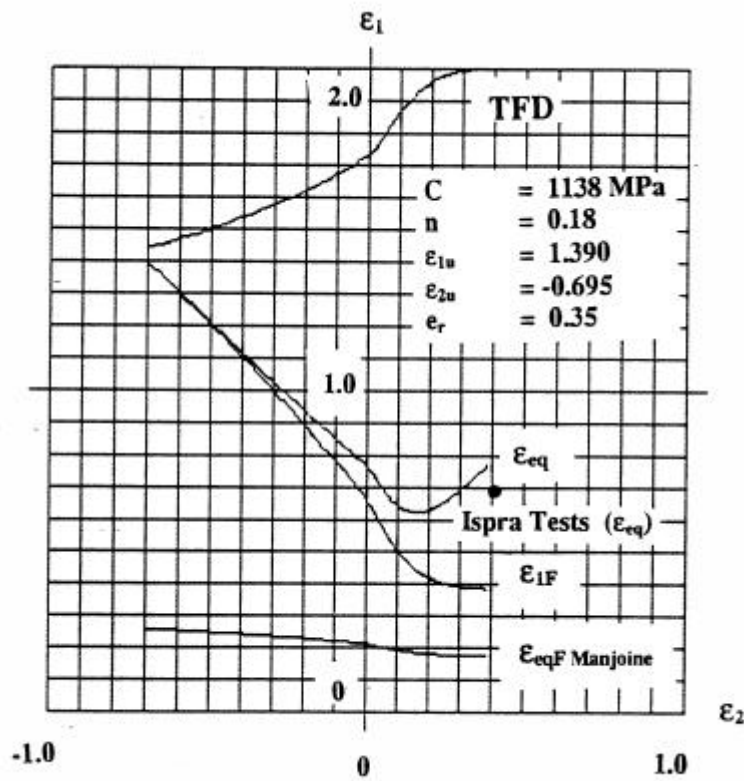


Fig. 3: Ghosh failure criteria applied to the Ispra tests material (Sa 537- Class 1)

What is shown by this family of curves is that for a given value of the TFD many different stress states exist. For example, plane stress conditions are obtained for $x=0$ or $y=0$, perfect triaxiality for $x=1$ and $y=1$, while plane strain, assuming proportionality between plastic strains and stress deviatorics, is obtained for $y = 2x-1$ or $y = \frac{1}{2}(x+1)$. During the test the stress path followed at a given material location can be drawn on the x - y plane to show how the stress state and the TFD value variate under increasing loads. The theories concerning the ductility reduction under triaxial conditions are based on a void growth whose rate depend on the instantaneous value of the TFD. So really what is relevant to produce the rupture at a given material location is the history of the TFD at that location. If the dependence on other parameters is excluded the knowledge of this history should be sufficient to determine when the rupture is approached at the considered location. It is evident, however, that from the experimental point of view, to exclude the dependence of the void growth on other parameters, tests based on the same TFD values but with different stress conditions should be performed. This is made complicate if the TFD during the test does not remain constant and is subjected to large variation.

FINAL REMARKS

Presently, investigations are carried out at the Catania University to clarify the TFD-ductility reduction curve. Also at the Cassino University an experimental campaign has been initiated on behalf of ANPA and theoretical-experimental investigations have been already carried out in the past (Bonora, 1996). Tests on biaxial specimens under dynamic conditions are performed at the Ispra JRC Laboratories. It is expected that this effort

will be increased in the future to fully clarify the material behavior in the whole range of possible conditions.

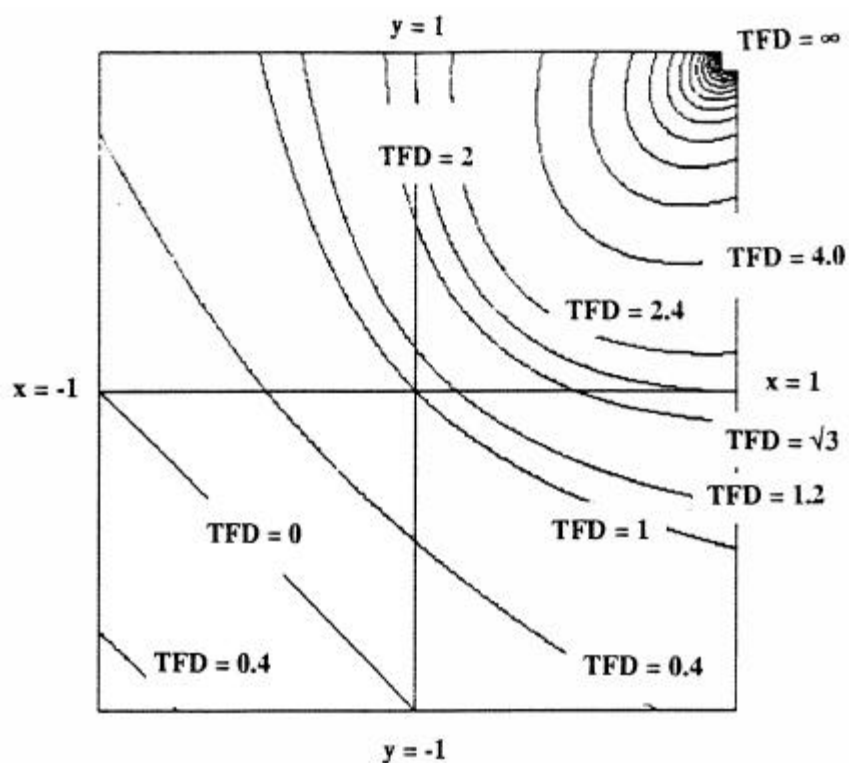


Fig. 4: Iso-TFD curves.

The authors are grateful to Dr. Carlo Albertini of the Ispra JRC Laboratories for his direction of the experimental campaign on cruciform specimens.

REFERENCES

- Bonora, N., 1996, "Effect of Triaxial State of Stress on Ductile Failure Damage Parameters", Eng. Fracture Mechanics.
- Dameron, R. A., Dunham, R. S., Rashid, Y. R. and Tang, H. T., 1991, "Conclusions of the EPRI Containment Research Program", Nuc. Engn. Des., Vol. 125, pp. 41-55.
- Ghosh, A. K., 1976, "Criterion for Ductile Fracture in Sheets under Biaxial Loading", Metallurgical Trans. A, Vol. 7A, pp. 523-533.
- Gurson, A. L., 1977, "Continuum Theory of Ductile Rupture by Void Nucleation and Growth: Part I - Yield Criteria and Flow Rules for Porous Ductile Media", J. Engn. Mat. Tech., Vol. 99, pp. 2-15.
- Manjoine, M. J., 1982, "Creep-Rupture Behavior of Weldments", Weld. Research Supplement (February 1982), pp. 50s-57s.
- McClintok, F. A., 1968, "A Criterion for Ductile Fracture by Growth of Holes", Journal of Applied Mechanics.
- Rice, J. R., Tracey, D. M., 1969, "On the Ductile Enlargement of Voids in Triaxial Growth Holes", J. Mech. Phys. Solids, Vol. 17, pp. 210-217.